A particular case of exotic resonant states: di-nuclear parent quasimolecular states

N. Grama, C. Grama, I. Zamfirescu

Horia Hulubei Institute of Physics and Nuclear Engineering, P.O.Box MG-6, Bucharest, Romania

Abstract

The properties of the parent quasimolecular states are deduced from the general properties of the exotic resonant states found by the Riemann surface approach to S-matrix poles.

1 Introduction

Di-nuclear quasimolecular states (QMS) represent the most important cluster phenomenon in nuclear physics. They are nuclear resonant states (RS) excited in heavy-ion reactions, having special properties: *a)* QMS are highly excited RS in nuclei above the threshold E_{th} of two-body decay into the cluster constituents; *b)* The reduced width of QMS for decay into cluster constituents is large, while the reduced widths for decay into other channels are small; *c)* QMS have good spins and parities (J^π); *d)* QMS excitation energies are situated around the top of the total barrier ($E^J_{QMS} \simeq E_{coul} + E_{centrifugal}$), in a region of high level density. Their widths Γ_{QMS} are of the order of hundred of keV; *e)* For a given J there are several QMS. The energy centroids of QMS with the same J form a straight line in the plane E_{ex} vs $J(J+1)$, appropriate to a rotational band.

As suggested by Feshbach [1] the narrow QMS with the same J^π are fragments of a di-nuclear parent quasimolecular state (PQMS) of a given J^π, as illustrated in fig. 1.

In spite of the great deal of research work done in the field of QMS there are main open questions still left [2] :

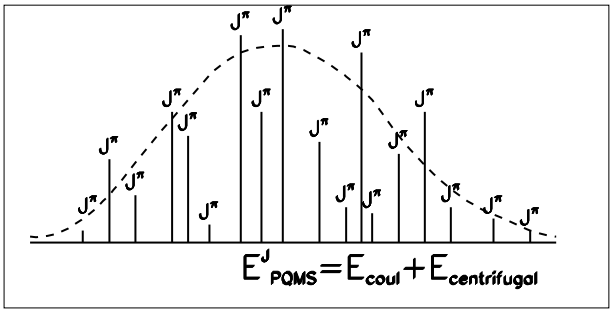

Figure 1: A di-nuclear PQMS with a width of several MeV (dashed line) is fragmented into a number of narrow QMS (having widths of order of hundreds of keV) with the same J^π.

Stability against the dissolution into the complex neighboring compound nuclear states: Because of the very high level densities at the excitation energies of QMS it is expected that QMS be totally damped, and consequently unobservable in the experiment. The fact that QMS have been observed in a region of high level density suggests that they belong to a new class of states of the nuclear system, that fulfil extraordinary conditions which prevent them from spreading out. The nature of the structural difference between the QMS and the underlying compound nuclear states should be explained.
The QMS wave function is localized in the barrier region: It is a great puzzle to understand how a short range nuclear attraction can be operative in order to generate a RS having the wave function localized outside the potential well, in the region of the barrier. For example, in the $^{12}C+^{12}C$ system the distance of the closest approach at a CM energy of 5.6 MeV (the lowest energy at which resonances have been observed) is 9.3 fm, while the ^{12}C radius is 3 fm. This means that the surfaces of the two nuclei will be separated by 3.3 fm in the closest proximity [3]. How could a short range attractive potential of about 4 fm (see fig. 2) be operative in this configuration, leading to the formation of a RS? Some attempts have been done to construct an attractive long range "effective" potential that could operate at the distance of the closest approach [3, 4], but this potential contradicts the usual potential shape. As shown in [5, 6] the large diffuseness used in [3, 4] decreases the Coulomb barrier so that the states are located above the barrier and consequently they are echoes and not RS.

The present work answers the above questions. By using an usual potential we are looking for the possibility to generate a class of exotic RS (ERS)

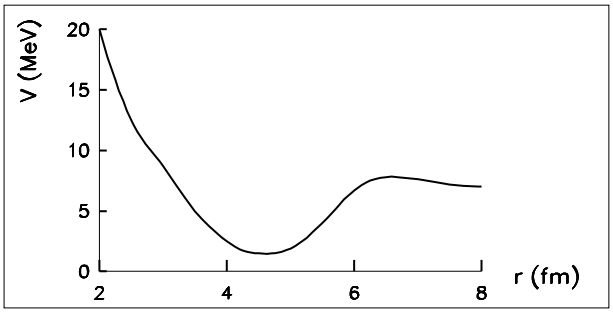

Figure 2: The potential for the $^{12}C + ^{12}C$ scattering in the s state

that could be candidates for PQMS, i.e. RS which have the wave function localized in the region of the barrier, particularly stable with respect to the dissolution into the neighboring compound nucleus resonant states. In order to do this we have to identify all classes of RS and to study their properties.

The existence of different types of RS must be reflected in the existence of different types of S-matrix poles. Consequently it is important to find a method to identify simultaneously all the S-matrix poles. Let us consider the non-relativistic scattering of a charged particle by a central potential

$$\mathcal{V}(r) = gV_n(r) + V_{bar}(r) \tag{1}$$

where the short range complex nuclear potential V_n of strength $g \in \mathbf{C}$ has a square or a Woods-Saxon form-factor, and V_{bar} is a potential barrier. The dimensionless variable r/R will be used instead of r. For the sake of simplicity the notation r, k, g and c will be used for the dimensionless variables r/R, kR, $(\hbar^2/2MR^2)g$ and cR (where c is the Coulomb parameter $c = Z_1Z_2e^2M/\hbar^2$). The S-matrix poles are the solutions $k = k_l(g)$ of the equation

$$\mathcal{F}_{l+}(g, k) = 0 \tag{2}$$

where $\mathcal{F}_{l+}(g, k)$ is the Jost function [7], l is the orbital angular momentum, k is the wave number and g is the potential strength, provided that $\mathcal{F}_{l-}(g, k) \neq 0$. The pole function $k = k_l(g)$ is a multiple-valued function defined on the complex g-plane. The S-matrix poles distribution in the k-plane as a function of the potential strength g has been extensively studied [8], [9], [10], [11], [12], [13] by using the *pole trajectory method*: a particular path in the complex g-plane is chosen and the corresponding trajectory of the S-matrix poles in the k-plane is determined. The pole trajectory method suffers from a poor

treatment of the multiformity of the function $k = k_l(g)$: the method does not provide all S-matrix poles, some important S-matrix poles being lost, and one can never be sure that the same pole is followed.

In order to get a better description of the function $k = k_l(g)$ the *Riemann surface approach to S-matrix poles* [14, 15, 16] will be used. It consists in constructing the Riemann surface $R_g^{(l)}$ over the g-plane, on which the pole function $k_l(g)$ is single valued and analytic. Each sheet is associated with one branch of the function. In other words if g takes a value on a sheet, then the function $k_l(g)$ takes only one value on the image of that sheet. The changes from one branch of the function to another are effected by making the g-variable change from one sheet to another. This is possible at the branch-points, i.e. at some special points on the Riemann surface that are common to different sheets. Two sheets are connected along the branch line that joins the common branch-points. A schematic illustration of the method is given in fig. 3.

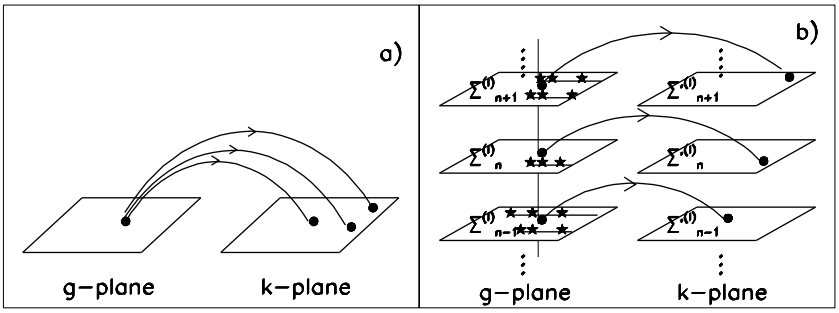

Figure 3: a) The multiple-valued function $k = k_l(g)$ defined on the complex g-plane and its distinct values in the k-plane. b) The Riemann surface over the complex g-plane. The branch-points indicated by $*$ and the branch-lines that join the sheets are shown. One can see that if g takes a value on a sheet $\Sigma_n^{(l)}$, then the function $k = k_l(g)$ takes only one value on the image of this sheet $\Sigma_n^{\prime(l)}$.

In fig. 3a) the function $k = k_l(g)$ defined on the complex g-plane is multiple-valued, i.e. there are many k values that correspond to the same value g. In fig. 3b) the sheets of the Riemann surface over the g-plane and their images in the k-plane are represented. Having located the branch points in the g-plane, cuts have been taken in the g-plane along the branch-lines. In this way all the sheets $\Sigma_n^{(l)}$ of the Riemann surface $R_g^{(l)}$ have been separated. One can see that if g takes a value on a sheet $\Sigma_n^{(l)}$, then the function $k = k_l(g)$ takes only

one value on the image of this sheet $\Sigma_n'^{(l)}$. In this way the function $k = k_l(g)$ defined on the Riemann surface $R_g^{(l)}$ becomes a single-valued function and it is no longer a multiple-valued function as it was while defined on the complex plane $g \in \mathbf{C}$. The border of any sheet image in the k-plane $\Sigma_n'^{(l)}$ was obtained by letting g trace a path along the cuts on the corresponding Riemann sheet $\Sigma_n^{(l)}$, without crossing them, and along a circle of large radius joining the cuts. Taking into account that one branch and only one branch of $k = k_l(g)$ is associated with a sheet $\Sigma_n^{(l)}$, the label n of this sheet will be used as a quantum number for the S-matrix pole belonging to the corresponding sheet image $\Sigma_n'^{(l)}$ in the k-plane and for the associated resonant (bound) state. This quantum number is important because it allows to label even the poles that do not become bound state poles as the depth of the potential well is increased. In the case when there are poles which do not become bound state poles as the depth of the potential well is increased the usual manner of labeling the resonant state poles by the same radial quantum number as the bound state poles into which they are transformed by increasing the strength of the potential well does not work. The label n of a Riemann sheet provides a unique quantum number for the resonant (bound) state pole that belongs to the corresponding Riemann sheet image. It does not change when the potential strength is changed taking values on the same Riemann sheet. For each l value all the S-matrix poles $k_l(g)$ have been found by constructing the Riemann surface $R_g^{(l)}$ over the g-plane on which the function $k = k_l(g)$ is single valued and analytic, and by constructing the images of the Riemann sheets in the k-plane [14, 15]. The method has been used for various shapes of potentials represented in fig. 4: a rectangular well followed by a rectangular barrier (fig. 3a), a rectangular or Woods-Saxon well with centrifugal barrier (fig. 4b) and a rectangular or Woods-Saxon well with Coulomb and centrifugal barrier (fig. 4c).

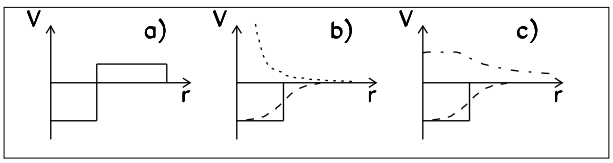

Figure 4: Three shapes of the potential for which the analysis of the Riemann surface has been done: a) a square well followed by a square barrier; b) a square or Woods-Saxon well with centrifugal barrier; c) a square or Woods-Saxon well with Coulomb barrier

2 Properties of the exotic resonant poles and states

For all mentioned potential shapes given in fig. 4 a new class of poles, with unusual properties, has been identified. The exotic resonant state poles have the following unusual properties:

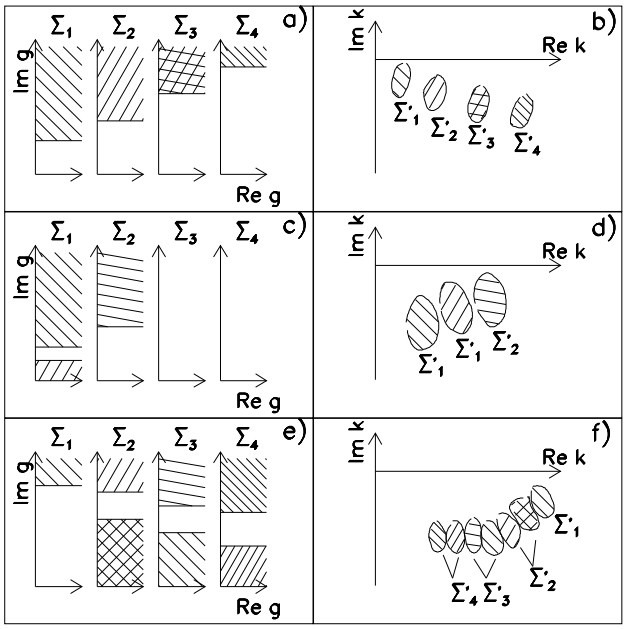

Figure 5: The first four sheets Σ_n, $n = 1, 2, 3, 4$ and the aggregates of their k-plane images Σ'_n for the three shapes of the potential given in fig. 4. In fig. 5a and 5b the sheets and the aggregate of the sheet images for the potential represented in fig. 4a are given; in fig. 5c and 5d the sheets and the aggregate of the sheet images for the potential represented in fig. 4b are given; in fig. 5e and 5f the sheets and the aggregate of the sheet images for the potential represented in fig. 4c are given.

(i) Instead of becoming bound or virtual state poles when the strength of the potential well increases to infinity, the exotic poles remain in some bound regions of the k-plane, in the neighborhood of some attractors (stable points). The number and position of these bound regions depend on the shape and height of the barrier. They occur only if the absorptive potential strength $\mathcal{I}m\ g > 0$ belongs to a certain window ($t_1 \leq \mid \mathcal{I}m\ g \mid \leq t_2$). Exotic poles exist only on some Riemann sheet images, depending on the shape of the

potential barrier, as illustrated in fig. 5. One can see that for a rectangular well followed by a rectangular barrier there are exotic poles only for strong absorptive potentials. There is an infinite number of Riemann sheet images on which there are situated exotic poles. On each Riemann sheet image there is only one bound region for the exotic resonant pole (see fig 5a and 5b). In the case of a rectangular or Woods-Saxon well with centrifugal barrier there are exotic poles on a finite number of Riemann sheet images, the number of these sheet images increasing as the orbital angular momentum l increases. The exotic poles occur for either weak or strong absorptive potentials (see fig. 5c and 5d). In the case of a rectangular or Woods-Saxon well with Coulomb plus centrifugal barrier there is an infinite number of Riemann sheet images where the exotic poles are situated, and the exotic poles occur for either strong or week absorption (see fig. 5e and 5f).
(ii) The wave functions of the RS corresponding to poles situated in the neighborhood of the attractors are almost completely confined to the region of the barrier. The localization of the wave function in the case of potential (1) having the shape of a rectangular well followed by a rectangular barrier is illustrated in fig. 6.

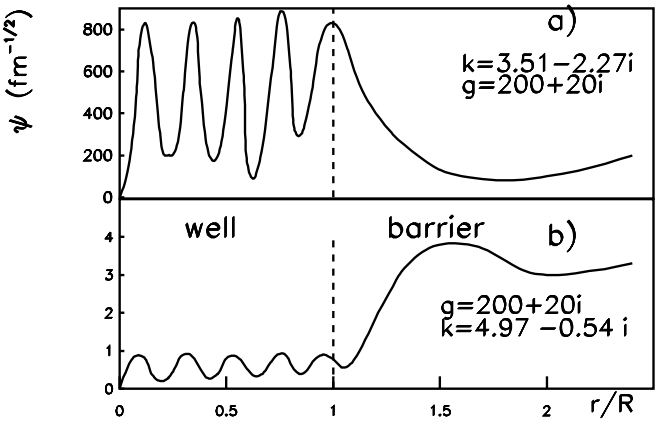

Figure 6: The moduli of the wave functions of an usual RS (a) and of an ERS (b) for the potential given in fig. 4a with equal radii for well and barrier. The values of the potential well depth g and the corresponding poles in the k-plane are given.

As a consequence of the localization of their wave functions the ERS are almost insensitive to the behavior of the potential inside the well, but almost totally determined by the potential in the barrier region.

3 Di-nuclear PQMS - a particular case of ERS

By comparing the properties of the ERS given above with the properties of the PQMS given in the Introduction we can conclude that the ERS are good candidates for PQMS. In the following we show that PQRS are a particular case of ERS, namely the ERS corresponding to poles located at the first attractor $k_z^{(1)}(c,l)$ for a potential made of a rectangular or Woods-Saxon well with Coulomb and centrifugal barrier. In the following we shall show that the properties of PQMS result naturally from the general properties of ERS for the mentioned potential.

3.1 Excitation energies

The ERS corresponding to poles at the first attractor $k_z^{(1)}$ form rotational bands. An approximation of the energy and width of these ERS has been obtained from the asymptotic expression of $k_z^{(1)}$ for large values of the Coulomb parameter c.

$$E \simeq \frac{\hbar^2}{2MR^2}\left\{k_B^2 - \alpha_1 X - \frac{\alpha_1^2}{2}\frac{X^2}{k_B^2} - \frac{\alpha_1^2 k_B^2}{2X}\right\} \tag{3}$$

$$\Gamma \simeq \frac{\hbar^2}{2MR^2}\left\{2\alpha_2 X - \alpha_1\alpha_2\frac{X^2}{k_B^2} - \frac{\alpha_1\alpha_2 k_B^2}{X}\right\} \tag{4}$$

where $k_B = [2c + l(l+1)]^{1/2}$; $X = [k_B^2 + l(l+1)]^{2/3}$; $\alpha_1 = Re\ \alpha$ and $\alpha_2 = Im\ \alpha$, with $\alpha = (9\pi/8)^{2/3}\exp(i\pi/3)$. The first term in (3) indicates a rotational character of the energy spectrum, while the other terms in (3) give corrections to the linear dependence of E on $l(l+1)$ and at the same time they show that the energy levels are situated below the barrier top $\hbar^2 k_B^2/2MR^2$. It results that both di-nuclear PQMS and ERS at the first attractor form rotational bands of simple configuration states at high energies in nuclei, near the top of the total barrier. A good agreement was obtained in the comparison of the theoretical energies given by (3) with the experimental energies of the PQMS reported in literature, from ^{12}C+^{12}C up to ^{28}Si+^{28}Si by using the same prescription for the radius $R = r_0(A_1^{1/3} + A_2^{1/3})$ with r_0=1.3 fm for all nuclear systems. The experimentally observed deviation from the linear dependence of E on $l(l+1)$ in the light systems, such as ^{12}C+^{12}C, ^{12}C+^{16}O and ^{16}O+^{16}O, results from the dependence of the slope

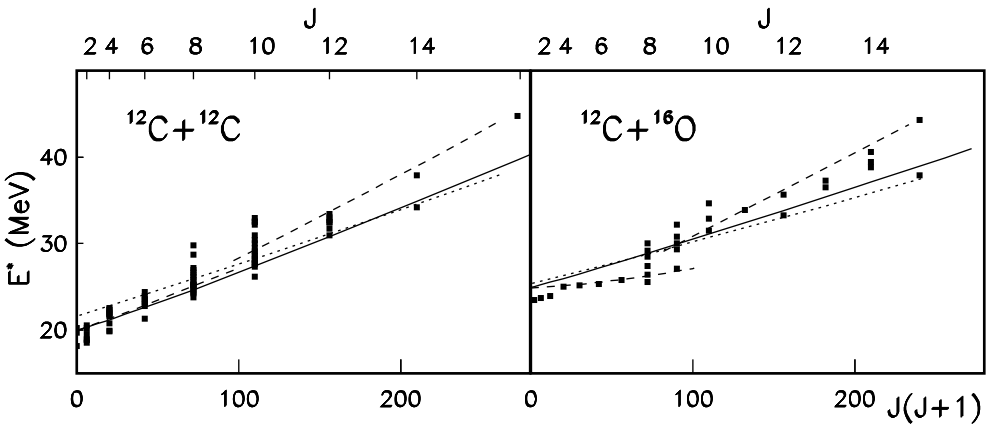

Figure 7: Comparison of the experimental excitation energies of PQMS with the ERS energies given by eq. (3) (continuous curves). The dot line is the grazing line. The dashed lines are the E vs $l(l+1)$ lines for different configurations (two separate spheres below the Coulomb barrier and two partially overlapping spheres above the Coulomb barrier).

of the tangent to the curve E vs $l(l+1)$ with respect to c and l. As one can see from Eq. (3), for light systems (small c) there is a rather strong variation of the slope with respect to l, especially for low l values.

Table 1: The separation distances between the centers of the two nuclei that form the di-nuclear PQMS. R_1 is the distance under the Coulomb barrier, and R_2 is the distance above the Coulomb barrier.

	[17]		[18]		Present paper
Nuclear system	R_1(fm	R_2(fm)	R_1(fm)	R_2(fm)	R(fm)
$^{12}C+^{12}C$	6.7	5.7	7.95	4.46	5.59
$^{12}C+^{16}O$	9.6	5.3	9.0	5.31	6.25
$^{16}O+^{16}O$			9.55	6.55	6.55

The calculated energies are obtained with the same radius prescription, both below and above the Coulomb barrier. Other authors [17], [18] have been forced to use two rotational bands for light heavy-ions systems, separated by the Coulomb energy E_{Coul}. In other words, these light systems (e.g. ^{12}C+^{12}C, ^{12}C+^{16}O and ^{16}O+^{16}O) were considered as di-nuclear systems of two separated spheres below the Coulomb barrier and of two partially overlapping spheres above the Coulomb barrier.

3.2 Widths

A comparison of the PQMS widths and ERS widths is difficult due to the process of spreading of the single particle excitation represented by the PQMS on a large energy region. It would be necessary to identify and analyze all the QMS of the same J^π that represent fragments of PQMS, spread on an energy interval of several MeV. As it can be seen from table 2 a good agreement was found between the calculated widths of the ERS given by eq.(4) and the experimental widths of the PQRM obtained by the reconstruction from the the available spread fragments [19], [20].

Table 2: Comparison of the PQMS widths and the ERS widths given by eq.(4)

Nuclear system	l	Γ_{PQMS} (MeV)	Γ_{ERS} (MeV)
$^{12}C+^{12}C$	4	7.6	8.2
	6	9.5	10.0
	8	14.9	12.3
$^{12}C+^{16}O$	7	12.1	10.6
$^{24}Mg+^{24}Mg$	34	19.0	25.3

3.3 Stability

The small amplitude of the wave function of an ERS inside the well leads to a small overlap with the adjacent RS of the continuum that are mostly confined to the compound nucleus radius, which is smaller than the potential well radius. In other words $< \psi_{ERS}|\psi_{CN} >$ is small. This small overlap confers stability to ERS against the dissolution into the complex neighboring compound nuclear states. The ERS are a new kind of doorway states, whose stability is a consequence of the localization of the wave function, rather than of a symmetry.

3.4 Observability

Eq. (4) provides information on the observability of QMS. For the light systems the width increases rapidly as l increases so that it becomes very large for a relatively low l value and the corresponding resonance in the cross section is not observed. For heavier systems the widths of ERS increase slowly as l increases and consequently the states can be observed even at

very large l values. For example, in the $^{12}C+^{12}C$ system the highest l-value of the observed quasimolecular resonance is l=18, while in the $^{28}Si+^{28}Si$ quasimolecular resonances with l=42 could be observed [21].

3.5 Potentials that support QMS

Systematic heavy ions scattering studies [22] have shown that an enhanced gross structure both in the angular distribution and excitation functions for light nucleus-nucleus systems is produced by a weakly absorbing four parameter optical potential of Woods-Saxon form. The absorption that explains the scattering data belongs to the absorption window that ensures the occurrence of the ERS.

4 Conclusions

It was shown that the di-nuclear parent quasimolecular state is an exotic resonant state that corresponds to a S-matrix pole in the neighborhood of an attractor in the k-plane. The properties of the PQRS (excitation energies, deviation from the linear dependence of excitation energies on $l(l+1)$, widths, stability, observability) result naturally from the general properties of the ERS. The open problems mentioned in connection with the PQRS are solved. The equations (3) and (4) have a predictive character, giving the energies and widths of the PQMS.

References

[1] H. Feshbach, J. Phys. (Paris) **C5**, Suppl 11, 177 (1976).

[2] N. Cindro, in *Nuclear Collective Dynamics*, Lectures of the 1982 International Summer school of Nuclear Physics, Poiana Brasov, Romania, World Scientific, p.397.

[3] L. Satpathy, in *Prog. in Particle and Nuclear Physics*, **29**, Pergamon Press, 1992, p.327.

[4] L. Satpathy, P. Sarangy, A. Faessler, J.Phys. G **12**, 201 (1986), J. Phys. G. **16**, 469 (1990).

[5] K. Kato and Y. Abe, Prog. Theor. Phys. **80**, 11 (1988).

[6] K. Kato and Y. Abe, Phys. Rev. C **55**, 1928 (1997).

[7] R. G. Newton, *Scattering Theory of Waves and Particles*, 2nd ed., Spriger Verlag, New York-Heidelberg-Berlin, 1982.

[8] E. M. Ferreira, A. F. F. Teixeira, J. Math. Phys. **7**, 1207 (1966).

[9] E. M. Ferreira, N. Guilen, J. Sesma, J. Math. Phys. **9**, 1210 (1968).

[10] S. Joffily, Nucl. Phys. A **215**, 301 (1973).

[11] L. P. Kok, H. van Haeringen, Ann. Phys.(N.Y.) **131**, 426 (1981).

[12] P. Kaus, C. J. Pearson, Nuovo Cimento **28**, 500 (1963).

[13] H. M. Nussenzveig , Nucl. Phys. **11**, 499 (1959).

[14] C. Grama, N. Grama, I. Zamfirescu, Ann. Phys. (N.Y.) **218**, 346 (1992).

[15] C. Grama, N. Grama, I. Zamfirescu, Ann. Phys. (N.Y.) **232**, 243 (1994).

[16] C. Grama, N. Grama, I. Zamfirescu, Phys. Rev. A **61**, 032716 (2000).

[17] D. A. Bromley, in *Proc. 4th Int. Conf. on Clustering Aspects of Nuclear Structure and Nuclear Reactions*, eds. J. S. Lilley, M. A. Nagarajan, Reidel, Dordrecht, 1985, p. 1.

[18] H. S. Khosha, S. S. Malik, R. K. Gupta, Nucl. Phys. A, **513**, 115 (1990).

[19] R. R. Betts, Nucl. Phys. A **447**, 257c (1985).

[20] H. Fröhlich et al., in *Lecture Notes in Physics* **156**, ed. Eberhardt K.A., (1982) p. 79.

[21] R. R. Betts, S. B. Di Cenzo, J. F. Petersen, Phys. Lett. B **100**, 117 (1981).

[22] R. H. Siemssen, in *Nuclear Molecular Phenomena, Proc. Int. Conf. on Resonances in Heavy Ions Reactions, Hvar, Yugoslavia*, eds. N. Cindro, 1977, p.79.